

OPTIMISATION AND ENHANCEMENT OF CRYSTALLINE NANOCELLULOSE PRODUCTION BY ULTRASONIC PRETREATMENT OF DISSOLVING WOOD PULP FIBRES

MAGDI GIBRIL,^{*,**} TAMRAT TESFAYE,^{***} BRUCE SITHOLE,^{*,****}
PRABASHNI LEKHA^{****} and DERESH RAMJUGERNATH^{*}

^{*}Department of Chemical Engineering, University of KwaZulu-Natal, Durban, South Africa

^{**}Faculty of Industrial Engineering and Technology, University of Gezira, Wad Medani, Sudan

^{***}Ethiopian Institute of Textile and Fashion Technology, Bahir Dar University, Ethiopia

^{****}Biorefinery Industry Development Facility, CSIR, Durban, 4041, South Africa

Received August 10, 2017

Cellulose degradation with sulphuric acid is widely used for the preparation of nanocellulose from wood fibres. However, the low-yield, the high concentration of sulphuric acid used and the long reaction time are major challenges in commercial production of crystalline nanocellulose using this process. In this study, ultrasonication was used as a pretreatment step to induce cavitation of cellulose in suspension. The idea was to break down the non-crystalline regions in cellulose, thus destroy the interfibrillar bonds between cellulose molecule layers, causing ‘cracking’ or ‘erosion’ on the cellulose surface. This would enhance the accessibility of the acid to the cellulose during the hydrolysis process, thus minimising the consumption of acid, energy, as well decreasing the hydrolysis time. The effect of ultrasonication time on the morphology, structure and properties of cellulose was investigated using SEM, XRD and TGA. SEM analysis showed ‘cracks’ on the surface of fibres for short treatment time (<5 minutes). Beyond this time, the surface morphology of cellulose fibres was totally changed into nanofibrils. XRD analysis indicated a marginal increase in the crystallinity index. TGA analysis showed that the pretreatment did not influence the thermal properties of cellulose. The extraction process of crystalline nanocellulose was further optimised using Response Surface Methodology/Box-Behnken design, with three levels and three variables: temperature, acid concentration and reaction time as independent variables, and percentage yield and particle size of crystalline nanocellulose as dependent variables. Regression equations were obtained to analyse the dependent variables and the optimum process parameters identified. From the results, it is evident that the ultrasonication pretreatment of dissolving wood pulp fibres results in enhanced generation of crystalline nanocellulose from the fibres.

Keywords: ultrasonication, pretreatment, crystalline nanocellulose, optimisation, dissolving wood pulp

INTRODUCTION

Cellulose is the most abundant polymer on Earth, representing 45% of the biomass. It is a linear homopolymer composed of 1-4 linked β -D-glucose units, which form long elementary fibrils that are linked together by intensive hydrogen bonds to form microfibrils.¹ Cellulose consists of crystalline domains (highly ordered microfibrils) and amorphous domains (randomly ordered microfibrils). The amorphous domains are relatively easy to remove *via* the hydrolysis process,² which results in a highly crystalline cellulose in the nanoscale range, *i.e.*, crystalline nanocellulose, cellulose nanowhiskers, cellulose nanofibrils *etc.* Nanocellulose is defined as

particles with at least one nanoscale dimension (1-100 nm), produced from a variety of cellulose sources, including bacteria, cotton, wood and agricultural waste *via* chemical, mechanical and biological methods, or by using a combination of these. Recently, nanocellulose has been used in applications such as gas barrier films, flexible displays, composites, functional papers, hydrogels *etc.*, mainly due to its unique properties, *i.e.*, low density, high strength and optical transparency, as well as renewability, biodegradability and low cost.^{3,4}

Cellulose hydrolysis with sulphuric acid has been used intensively to prepare nanocellulose

from lignocellulosic fibres. However, the low yield of nanocellulose, the high concentration of acid used and the long reaction time needed represent the main challenges for this technique. The degradation of cellulose with acid starts with the most accessible parts of the cellulose fibre (the amorphous regions), followed by reducing the end groups and then the surface of highly ordered crystalline regions.⁵ However, unlike the amorphous region, the hydrolysis of crystalline regions takes place under extreme conditions, such as high acid concentration, high temperature and long reaction time, *i.e.*, the crystalline regions limit the accessibility of the acid into microfibrils. Hence, acid concentration, reaction time and reaction temperature are the most important parameters for controlling the acid hydrolysis of cellulose fibre. Generally, the hydrolysis of cellulose with sulphuric acid has been optimised by using a 50-65 wt% sulphuric acid solution at 45-50 °C for 45-60 min under mechanical stirring in order to produce nanocellulose.^{6,7} However, the high concentration of corrosive sulphuric acid (60-65%) and the low yield of nanocellulose represent the main challenges for commercial production.

Ultrasonication (sonication) generates ultra-high frequency sound waves that alter the molecular structure of cellulose by cavitation. Cavitation initiates when the generated bubbles collapse after expanding to the maximum size at a localised temperature (approximately 5000 K) and high pressure (approximately 5000 kPa). Those energies are efficient in breaking down the non-crystalline regions (amorphous) and causing cracks on the surface of the crystalline region, *i.e.*, breaking down the interfibrillar bonding. Ultrasonication has been employed to prepare cellulose nanofibrils (NFC), which were combined with an acid medium for preparing crystalline nanocellulose (CNC).^{8,9} In another work, Wong *et al.*¹⁰ showed that ultrasonication has the ability to decrease the molecular weight of cellulose during the modification process.^{8,11} In other words, ultrasonication caused degradation of the polymers without changing their chemical properties. A high yield of CNC was successfully achieved from microcrystalline cellulose *via* sono-assisted TEMPO-oxidation, followed by a sonication process.¹²

The work reported here was designed to apply ultrasonication as a pretreatment step to induce cavitation in the cellulose fibres in order to break down the amorphous region into nanofibrils. This

pretreatment would decrystallize the crystalline region, causing cracking or erosion on the surface and would potentially enhance the acid accessibility during the hydrolysis. This could lead to minimising the consumption of acid, energy, as well as to decreasing the hydrolysis time.

EXPERIMENTAL

Materials

Dissolving pulp was obtained from a local pulp mill, sulphuric acid (99.8%) and regenerated cellulose dialysis tubes (12,000 Da MWCO) were purchased from Sigma-Aldrich (South Africa).

Experimental work

With the aid of the Design of Experiment software and statistical analysis, the required number of experimental runs was determined. The experimental design was differentiated into two parts, *i.e.*, A and B. Part A entailed using a single variable to investigate the effect of ultrasonication pretreatment time (0, 5, 15, 30 and 45 min) on the yield of CNC under common hydrolysis conditions (*i.e.*, concentration (65%), time (60 min) and temperature (45 °C)). Part B entailed the optimisation of the CNC production process by using statistically designed experiments.

Part A: Effect of ultrasonication time on yield of CNC

Table 1 lists the experimental runs; each run was performed in triplicate.

Ultrasonication

The experimental procedure followed for Part A was similar to the common procedure of acid hydrolysis reported in the literature, except for the addition of the ultrasonication pretreatment step before conducting the rest of the acid hydrolysis. The cellulose fibres were suspended in 500 ml deionized water and then ultrasonicated using a UP400S ultrasonic processor (OMNI International, Georgia, USA) at a frequency of 70 Hz and an amplitude of 75% for a prescribed pretreatment time (Table 1) in a cold water bath (temperature below 5 °C). The sample was then centrifuged for 10 minutes at 9000 rpm. The excess water was decanted and kept for further application (*i.e.*, to quench the hydrolysis reaction). The precipitated pulp after centrifugation was dried using a drying oven and the amount of cellulose removed *via* ultrasonication was calculated.

Acid hydrolysis

Dried ultrasonicated fibres were shredded and subjected to acid hydrolysis under the following conditions: contact time (60 min), temperature (45 °C) and acid concentration (65%). The reaction was quenched at room temperature after 60 minutes, then

centrifuged and dialysed for 5 days. Thereafter, the sample was ultrasonicated for 5 min. The ultrasonication time was kept constant for Part B of the experiment. The other process variables, such as hydrolysis temperature, acid concentration and hydrolysis time, were varied according to the experimental procedures developed.

Characterisation of ultrasonicated cellulose

The morphological structure of cellulose samples (before and after ultrasonication) was studied with scanning electron microscopy (SEM) (Carl Zeiss, Oberkochen, Germany). The cellulose fibres were coated with gold using a Polaron SC 500 gold coater. Transmission electron microscopy (TEM) was used to determine the dimensions of the CNC particles. A JEOL 2100 TEM (Brightfield, Darkfield, STEM, Diffraction – JEOL HRTEM 2100, Massachusetts, USA) was used to capture images at 100 kV. Coated

Cu grids were dipped in CNC suspension and left to air-dry for 30 min. It was thereafter negatively stained with 2% uranyl acetate for 10 min and allowed to dry at room temperature. X-ray diffraction (XRD) data were obtained using a Rigaku Ultima 3 X-ray instrument (Empyrean, PANalytical, Almelo, Netherlands) on samples prepared as powder. Ni-filtered CuK α radiation ($\lambda = 1.54060 \text{ \AA}$) generated at a voltage of 40 kV and current of 40 mA, at a scan speed of 5 °/min at 2θ from 5° to 60°, was used. The crystallinity index (Cr) was calculated from the height of 200 peaks (I_{200} , $2\theta = 22.6^\circ$) and the intensity between the height peaks of 200 and 110 (I_{am} , $2\theta = 18^\circ$) using Segal's empirical equation. Thermogravimetric analysis (TGA) was performed using a TA Instruments (Q500, NETZSCH, Boksburg, South Africa), under nitrogen gas purge and a heating rate of 5 °C min⁻¹.

Table 1
Experimental runs: Part A

Runs	Sonication time (min)	Acid concentration (%)	Hydrolysis time (min)	Hydrolysis temperature (°C)
Run 1	U-00	65	60	45
Run 2	U-05	65	60	45
Run 3	U-15	65	60	45
Run 4	U-30	65	60	45
Run 5	U-45	65	60	45

Table 2
Coded values of variables used in Box-Behnken design

Coded value	Independent variables	Level		
		-1	0	1
X ₁	Acid concentration (%)	45	55	65
X ₂	Temperature (°C)	45	50	55
X ₃	Time (min)	30	45	60

Acid hydrolysis

Dried ultrasonicated fibres were shredded and subjected to acid hydrolysis under the following conditions: contact time (60 min), temperature (45 °C) and acid concentration (65%). The reaction was quenched at room temperature after 60 minutes, then centrifuged and dialysed for 5 days. Thereafter, the sample was ultrasonicated for 5 min. The ultrasonication time was kept constant for Part B of the experiment. The other process variables, such as hydrolysis temperature, acid concentration and hydrolysis time, were varied according to the experimental procedures developed.

Characterisation of ultrasonicated cellulose

The morphological structure of cellulose samples (before and after ultrasonication) was studied with scanning electron microscopy (SEM) (Carl Zeiss, Oberkochen, Germany). The cellulose fibres were

coated with gold using a Polaron SC 500 gold coater. Transmission electron microscopy (TEM) was used to determine the dimensions of the CNC particles. A JEOL 2100 TEM (Brightfield, Darkfield, STEM, Diffraction – JEOL HRTEM 2100, Massachusetts, USA) was used to capture images at 100 kV. Coated Cu grids were dipped in CNC suspension and left to air-dry for 30 min. It was thereafter negatively stained with 2% uranyl acetate for 10 min and allowed to dry at room temperature. X-ray diffraction (XRD) data were obtained using a Rigaku Ultima 3 X-ray instrument (Empyrean, PANalytical, Almelo, Netherlands) on samples prepared as powder. Ni-filtered CuK α radiation ($\lambda = 1.54060 \text{ \AA}$) generated at a voltage of 40 kV and current of 40 mA, at a scan speed of 5 °/min at 2θ from 5° to 60°, was used. The crystallinity index (Cr) was calculated from the height of 200 peaks (I_{200} , $2\theta = 22.6^\circ$) and the intensity between the height peaks of 200 and 110 (I_{am} , $2\theta =$

18°) using Segal's empirical equation. Thermogravimetric analysis (TGA) was performed using a TA Instruments (Q500, NETZSCH, Boksburg, South Africa), under nitrogen gas purge and a heating rate of 5 °C min⁻¹.

Part B: Optimisation of CNC extraction

After having determined the best conditions of ultrasonication, the extraction process was further optimised using a Box-Behnken design, as shown in Table 2. The best ultrasonication pretreatment time (U-30) from Part A, based on the CNC yield, was selected as the constant parameter (variable) in Part B. A response surface methodology design with three independent variables (acid concentration (45-65%), time (30-60 min) and temperature (45-55 °C)), with a total number of 18 experimental runs, was employed. The coded values of the variables at various levels are given in Table 2. The percentage yield and the particle size of the extracted CNC were determined by the coefficient of determination, analysis of variance and contour plots.

RESULTS AND DISCUSSION

Ultrasonication is widely used in many industrial applications, such as cleaning, plastic welding and chemical reactivity.^{9,11} In this study, ultrasonication has been used to induce cavitation in a cellulose suspension. Ultrasonication creates air bubbles within the cellulose suspension and when the bubble volumes reach a maximum size, due to maximum energy absorption, they collapse. The collapse of the bubbles results in emission of high temperatures (approximately 5000 K) and high pressures (approximately 5000 kPa) for a relatively small amount of time. This energy is sufficient for the breakdown of amorphous and weakly bonded regions of cellulose fibres.⁸ Ultrasonication also causes surface erosion and fibrillation when applied to cellulose fibres. This could ultimately assist with enhanced acid penetration during further hydrolysis processes.⁸ During mechanical treatment (ultrasonication) of cellulose fibres, the non-crystalline region, interfibrillar molecules and interfibrillar bonds will break, creating fibrils in the nanometer size range (width and length) that are known as cellulose nanofibrils (CNF).⁷⁻¹² In the first set of experiments, the effect of ultrasonication time on CNC yield and its influence on the physicochemical characteristics of the cellulose fibre was investigated.

Effect of ultrasonication on CNC yield

The yield of CNC was calculated as a percentage of the ratio of the dry mass of CNC

(freeze-dried) to the initial dry mass of cellulose (dried). As can be seen in Table 3, the average CNC yield was 42.33% under standard conditions (U-00). The yield significantly increased to 51.53% after ultrasonication for 5 minutes, to 66.13% after 15 minutes, and reached a maximum of 79.54% after ultrasonication for 45 minutes. Literature data confirm that the high yields were due to the enhancement of acid accessibility by the ultrasonic pretreatment.⁹ This study demonstrates that applying ultrasonication as a pretreatment step to acid hydrolysis to produce CNC significantly increases the yields of the CNC produced.

Effect of ultrasonication on morphological structure of CNC

The morphological and structural changes of cellulose due to ultrasonication were examined by SEM (Fig. 1). Untreated cellulose fibres (Fig. 1A) exhibit a smooth surface. After ultrasonication for 5 minutes, cracks on the fibre walls are evident (Fig. 1B and C), indicating that the ultrasonication disturbed the hydrogen bonds on the surface layers (outer core) of the fibres. This probably occurred due to the collapse of bubbles and pressure variation induced by cavitation. The surface morphology of cellulose fibres changed significantly after longer ultrasonication times: there was extensive disruption of the fibre layers and it appeared as if the outer core peeled away and the inner core ruptured, suggesting a disruption of hydrogen and interfibrillar bonds between the cellulose layers (as demonstrated in Fig. 1D-F). The peeled core or layer (Fig. 1F) showed web-like cellulose fibrils and a tendency towards the formation nanofibrillated cellulose. SEM confirmed the cellulose fibre disruption due to ultrasonication by the observed peeling away fibril layer and the formation of the fibril web. This disruption may provide better accessibility of the acid during the hydrolysis process.

Effect of ultrasonication on crystalline structure of cellulose

The resultant XRD patterns are depicted in Figure 2. All XRD curves showed a typical cellulose I crystalline structure^{13,14} that exhibited characteristic peaks around 16° (110 plane) and 22° (200 plane) with varying intensities. The degree of crystallinity was calculated by using the empirical equation 1:¹⁵

$$CI = 100 \frac{I_{200} - I_{non-cr}}{I_{200}} [\%] \quad (1)$$

where CI expresses the apparent crystallinity [%] defined by Segal and co-workers,¹⁵ I_{200} gives the maximum intensity of the peak corresponding to the plane in the sample with the Miller indices 200 at a 2θ angle between 22-24°, and I_{non-cr} represents the intensity of diffraction of the non-

crystalline material, which is taken at an angle of about 18° 2θ in the valley between the crystalline peaks.

The results for the effect of ultrasonication on the degree of crystallinity of the cellulose samples are listed in Table 4. They indicate a slight decrease of the crystallinity index with an increase in ultrasonication time, in agreement with the results obtained by Wang *et al.*^{16,17}

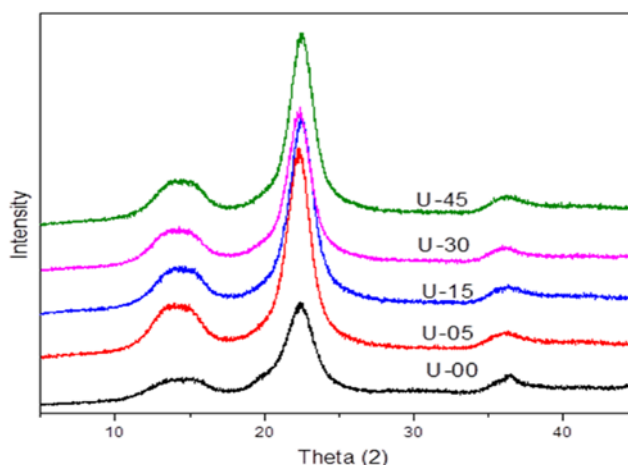


Figure 2: Effect of ultrasonication time on X-ray diffraction patterns of cellulose

Table 4
Effect of ultrasonication on crystallinity index

Samples	Sonation time (min)	Initial weight (g)	Weight after sonication	Weight loss (%)	Crystallinity index
U-00	00	5	5	0	72±1.61
U-5	5	5	4.696±0.130	6.08	71±1.03
U-15	15	5	4.513±0.109	9.74	71±0.99
U-30	30	5	4.493±0.211	10.10	69±1.09
U-45	45	5	4.433±0.231	11.34	67±1.11

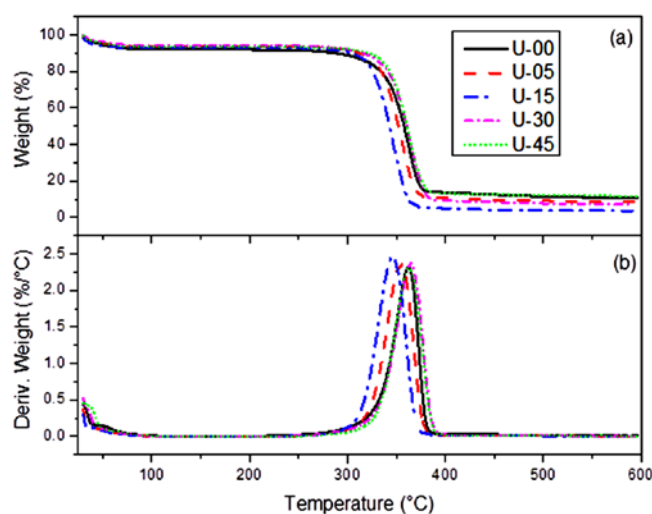


Figure 3: Effect of ultrasonication time on TGA and DTG profiles of cellulose

Table 3
Yield of CNC as a function of ultrasonication pretreatment time (Part A)

Ultrasonication time (min)	Acid conc. (%)	Hydrolysis time (min)	Hydrolysis temp. (°C)	Initial mass (g)	Mass after ultrasonication (g)*	Sonication yield (%)	Total yield (%)
U-00	65	60	45	5	5	0	42.32
U-05	65	60	45	5	4.696±0.13	6.08	51.53
U-15	65	60	45	5	4.513±0.109	9.74	66.13
U-30	65	60	45	5	4.493±0.211	10.10	77.69
U-45	65	60	45	5	4.433±0.231	11.34	79.54

*The mass is the average value of at least 4 repeated measurements

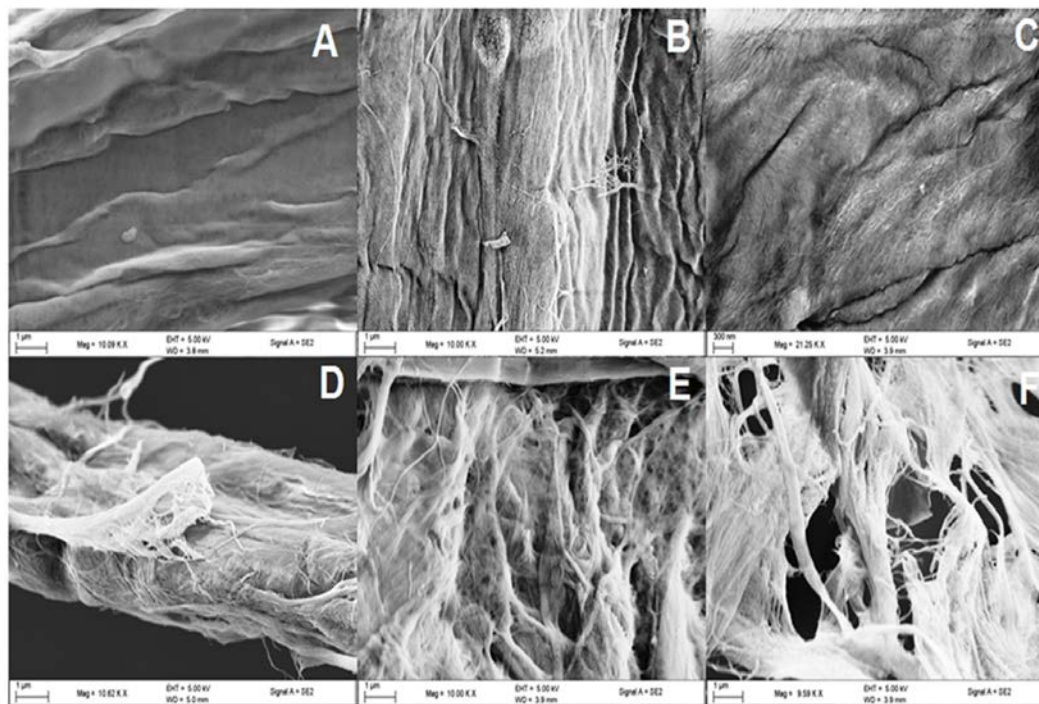


Figure 1: SEM images of initial sample (A) and sonicated ones for 5 min (B), 10 min (C), 15 min (D), 30 min (E) and 45 min (F)

Effect of ultrasonication on thermal properties of CNC

Figure 3 (a and b) shows the TGA and DTG curves of cellulose (U-00) and ultrasonicated cellulose (U-05, U-15, U-30 and U-45) over the temperature range of 30 to 600 °C. All the samples exhibited a small weight loss below 110 °C due to the evaporation of water. However, there was a small variation in the degradation behaviour at higher temperatures. The untreated sample (U-00) showed a single step pyrolysis within the 240–383 °C temperature range. This is associated with thermal degradation of cellulose. The degradation of ultrasonicated cellulose samples (U-05, U-15, U-30 and U-45) displayed similar thermal degradation behaviours in a slightly lower pyrolysis temperature range – of 250–365 °C. From the DTG curves, the maximum mass loss of untreated cellulose (U-00) appeared at 363 °C, which is related to the decomposition of the cellulose polymer. In ultrasonicated samples U-05 and U-15, the temperature of the maximum mass loss was shifted to lower values – of 356 °C and 347 °C, respectively. This indicates that the hydrogen bonds were disrupted. Samples U-30 and U-45 exhibited the same temperature of the maximum mass loss as the U-00 sample. It appears that, upon long durations of ultrasonication treatment, portions of the amorphous cellulose turned into nanofibrils, which are characterised by high surface area due to increased hydrogen bond interactions. These results are consistent with SEM observations.

$$\begin{aligned} (\text{Yield})^{-0.51} = & -0.22627 + 0.013701 * \text{temperature} - 4.61684\text{E} - 003 * \text{acid concentration} + 4.48133\text{E} - 004 * \text{time} \\ & - 1.828\text{E} - 006 * \text{acid concentration} * \text{temperature} - 1.7599\text{E} - 006 * \text{acid concentration} * \text{time} \\ & - 1.3403\text{E} - 004 * \text{temperature}^2 + 4.4666\text{E} - 005 * \text{acid concentration}^2 - 7.3909\text{E} - 006 * \text{time}^2 \end{aligned}$$

The analysis of variance (ANOVA) (Tables 6 and 7) indicated that this regression model was extremely significant ($P < 0.000000001$). As shown in Tables 6 and 7, the F value and p value for the lack-of-fit test were 100.82 and 0.0000007, respectively. This implies that time was the most significant variable and indicates that the model equation was adequate for predicting the CNC extraction. The linear acid concentration F value and P value were 78.00 and 0.0000025, respectively, which implies that the acid concentration was the second most significant variable. The fitness of the

Effect of ultrasonication on TEM images of cellulose

Transmission electron microscopy (TEM) analysis was performed to investigate the size of the resultant CNC fibres. Figure 4 (A, B, C and D) presents TEM images of untreated cellulose (U-00), and correspondingly of the samples pretreated for 15 min (U-15), 30 min (U-30) and 45 min (U-45). The results show that CNCs of different lengths and widths were obtained, depending on the ultrasonication times – longer pretreatment times led to fibres of shorter lengths and higher homogeneity. The number of CNC rods and their dimensions, such as length and diameter, were obtained from the SEM images.

Optimisation of CNC extraction using a Box-Behnken design

Eighteen (18) experimental runs were conducted to optimise the percentage yield and particle size of the extracted CNC based on three independent variables (temperature, acid concentration and time) (Table 5).

Optimisation of CNC yield

Fitting the models. The independent variables (acid concentration, temperature and time) and the dependent variable (yield) were analysed to obtain a regression equation, *i.e.*, an empirical relationship between the CNC yield and the test variable in coded units, which could predict the response under the given range. The regression of the factorial equation obtained for the extracted CNC yield was as follows:

model was further confirmed by a satisfactory value of the determination coefficient, calculated to be 0.96, indicating that 96% of the variability in the response could be predicted by the model. The value of the adjusted determination coefficient (adjusted $R^2 = 0.94$) also confirmed that the model was highly robust.

The optimisation studies indicated that the effects of both the linear and interaction effects of time, acid concentration and temperature on the CNC yield were statistically significant. Figure 5 shows the three-dimensional surface

plot of the optimisation process. The results in Figure 5 reveal that the increase of each factor improves the CNC yield. Also, the increase in the interaction effects (temperature *vs.* time, time *vs.* acid concentration, and temperature

vs. acid concentration) results in an increment in the CNC yield. The results demonstrate that generally the yield is higher at a higher temperature, higher concentration and higher treatment time.

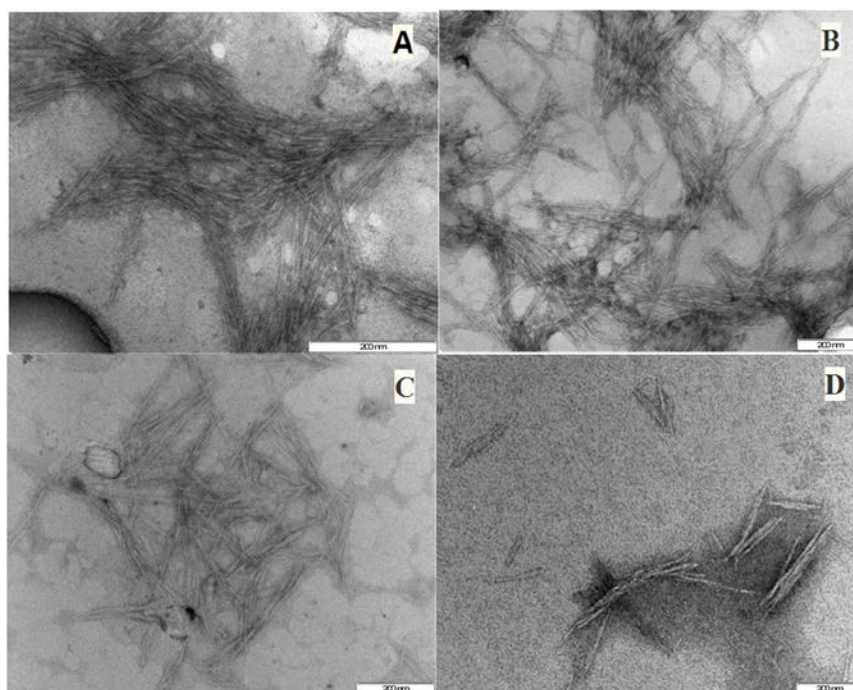


Figure 4: TEM images of CNC prepared with different sonication duration; U-00 (A), U-15 (B), U-30 (C) and U-45 (D)

Table 5
Experimental runs developed for Part B

Run	Pretreatment time	Temp. (°C)	Acid conc. (%)	Time (min)	CNC size	Yield (%)
1	U-30	40	45	45	3000	8.99
2	U-30	40	55	30	2800	11.5
3	U-30	40	55	60	610	30.1
4	U-30	40	65	45	405	37.3
5	U-30	45	45	60	570	41.3
6	U-30	45	45	30	800	13.6
7	U-30	45	55	45	550	29.3
8	U-30	45	55	60	310	54.13
9	U-30	40	45	60	800	20.9
10	U-30	45	45	45	900	18.7
11	U-30	45	65	60	270	71.79
12	U-30	45	65	30	590	47.91
13	U-30	50	45	45	600	33.7
14	U-30	50	55	60	350	59.5
15	U-30	50	55	30	1100	28.35
16	U-30	50	65	60	190	78.98
17	U-30	50	65	45	210	73.61
18	U-30	50	65	30	479	44.1

Diagnostic plots were drawn to judge the model adequacy in the experimental data. The plot of the observed response (CNC yield) *versus* the predicted response is shown in Figure 6. The results in Figure 6a confirm the correlation between the actual and the predicted values. In this case, the predicted values agreed with the observed ones in the range of the operating variables. The normal probability plot of the studentised residuals was used to check for normality of residuals (Fig. 6). The linear pattern observed in this

plot suggests that there was no sign of any problem in the experimental data. Residuals displayed randomness in scattering and suggested that the variance of the original observation was constant. The linear correlation plot drawn between the predicted and experimental value demonstrated a high R^2 value (0.96), indicating excellent fit ($p < 0.0000001$). Thus, the low magnitudes of error, as well as the significant values of R^2 in the yield optimisation of the extracted CNC, prove the high prognostic ability of the model.

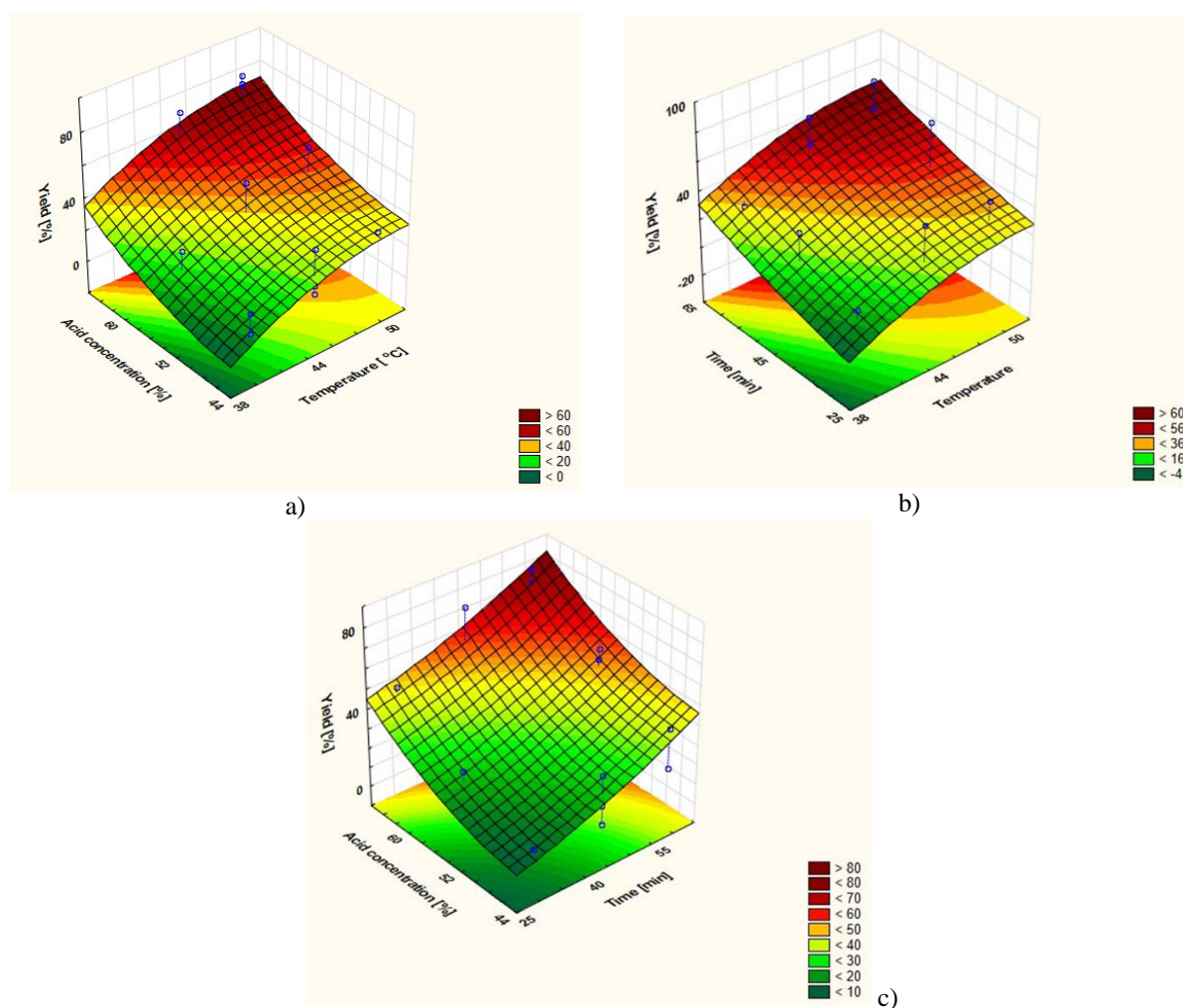


Figure 5: Response surface plot showing the effect of (a) acid concentration and temperature, (b) time and temperature, and (c) acid concentration and time on percentage yield

Regression analysis (Table 8) and Pareto chart (Fig. 6) results indicate that temperature is the first most influencing variable and time is the second one among the chosen parameters, as indicated by the p values. The significance of each coefficient was determined using the Pareto chart and p value in Table 8 and it could be easily noticed that the variable with the largest effect was the

linear term of temperature, followed by the linear time and the linear acid concentration. The factor t-test value (10.04) and p value (0.000000709) correspond to linear time, t-test value (8.83) and p value (0.000002519) correspond to linear acid concentration and t-test value (7.44) and p value (0.000012844) correspond to linear temperature.

Table 6
Effect estimates of a full second-order polynomial model for optimisation of CNC yield

Factor	Dependent variable = Yield; $R^2 = 0.96$; Adjusted $R^2 = 0.94$; MS Residual = 28.10					
	Effect	Standard error	T	P	-95% Confidence limit	+95% Confidence limit
Mean/intercept	36.63	1.27	28.74	0.000000001	33.82	39.43
Temperature (°C) (L)	24.85	3.33	7.44	0.000012844	17.50	32.20
Temperature (°C) (Q)	4.34	2.61	1.65	0.125429737	-1.42	10.11
Acid concentration (%) (L)	27.64	3.13	8.83	0.000002519	20.75	34.53
Acid concentration (%) (Q)	-1.88	2.80	-0.67	0.515736834	-8.06	4.29
Time (min) (L)	32.58	3.24	10.04	0.000000709	25.44	39.72
Time (min) (Q)	-5.65	2.76	-2.04	0.06538148	-11.73	0.42

Table 7
ANOVA of a full second-order polynomial model for optimisation of CNC yield

Factor	Dependent variable = Yield; $R^2 = 0.96$; Adjusted $R^2 = 0.94$; MS Residual = 28.10				
	SS	Df	MS	F	p
Temperature (°C) (L)	1557.78	1	1557.78	55.43	0.0000128
Temperature (°C) (Q)	77.29	1	77.29	2.75	0.1254297
Acid concentration (%) (L)	2191.91	1	2191.91	78.00	0.0000025
Acid concentration (%) (Q)	12.67	1	12.67	0.45	0.5157368
Time (min) (L)	2833.12	1	2833.12	100.82	0.0000007
Time (min) (Q)	117.67	1	117.67	4.18	0.0653814
Temperature (°C) L+Q	1616.56	2	808.28	28.76	0.0000426
Acid concentration (%) L+Q	2262.44	2	1131.22	40.25	0.0000087
Time (min) L+Q	2996.75	2	1498.37	53.32	0.0000021
Error	309.10	11	28.10		
Total SS	7990.53	17			

Square values of the variables are used to indicate their quadratic effects, so as to get the curvature in the response surface graphs and to get the optimal value for each variable. The fit of the model was checked by the coefficient of determination (R^2), which is 0.96, and this revealed that 96% of the sample variation in CNC yield is attributed to independent variables.

Optimisation of particle size of the extracted CNC

Fitting the models. The independent and dependent variables were analysed to obtain a

$$\begin{aligned} (\text{CNC size})^3 = & -4.29924 + 0.18305 * \text{Temperature} + 0.022453 * \text{Acid concentration} + 0.014082 * \text{Time} - 7.1811\text{E} \\ & - 004 * \text{Temperature} * \text{Acid concentration} - 4.95633\text{E} - 005 * \text{Temperature} * \text{Time} - 2.14842\text{E} \\ & - 004 * \text{Acid concentration} * \text{Time} - 1.36463\text{E} - 003 * \text{Temperature}^2 + 2.77278\text{E} - 004 \\ & * \text{Acid concentration}^2 + 7.11284\text{E} - 005 * \text{Time}^2 \end{aligned}$$

The analysis of variance (ANOVA) (Tables 9 and 10) indicated that this regression model was extremely significant ($P < 0.00006$). The lack of fit test measures the failure of the model to represent the data in the experimental domain at points which are not included in the regression. As shown in Tables 9 and 10, the F value and p value for the lack-of-fit test were 5.9 and 0.032, respectively. This implies that the temperature was the most significant independent variable and indicates that the model equation was adequate for predicting the size of CNC. The second significant independent variable was time with a 5.853 F value and 0.033 p value. The acid concentration was, however, not a significant variable for CNC size determination. The fitness of the model was further confirmed by a satisfactory value of the determination coefficient. This was calculated to be 0.63, indicating that 63% of the variability in the response could be predicted by the model. The value of the adjusted determination coefficient (adjusted $R^2 = 0.43$) also confirmed that the model was robust.

The optimisation studies indicated that the effects of acid concentration, treatment time and temperature on the particle size of the extracted CNC were statistically significant and there were significant relations of the variables for CNC size. Three-dimensional (3D) contour plots were generated by Statistica 13 software. In general, the 3D plots show the overall contribution of temperature, time, acid concentration (independent variables) to the CNC size. The green region signifies that the

regression equation. This was an empirical relationship between the CNC size and the test variable in coded units, and it could predict the response under the given range. Independent and dependent variables were analysed to get the regression equations that could predict the response under the given range. Each of the observed values was compared with the predicted value calculated from the model. The regression quadratic equation obtained for the CNC size was as follows:

independent factors had a high impact on the CNC size reduction. The significance of independent variables increases with the intensification of colourisation from the dark red region to the dark green region progressively. The stationary point, which is denoted by the dark green region on the lower part of the wedge-like 3D plot is the optimised point. Hence, it can be justified that the acid concentration and temperature (Fig. 7a), time and temperature (Fig. 7b) and acid concentration and time (Fig. 7c) are critical parameters in altering the size of CNC. At low acid concentration, low temperature and minimum time of extraction, the size of CNC is the highest throughout the 3D contour plot. This result is valid as all the independent variables (acid concentration, time and temperature) had to perform their function in isolating the CNC. Without sufficient acid concentration, time of treatment and temperature of treatment, the particle size of the extracted CNC will be affected, resulting in a higher particle size. Figure 7a signifies the pattern changes as the temperature of treatment increases with increasing the acid concentration. This produces a lower particle size of the extracted CNC.

Figure 8 illustrates the correlation of the actual value to the predicted value. For validation of the results, the experimental values of the response were compared with the anticipated values and the percentage prediction.

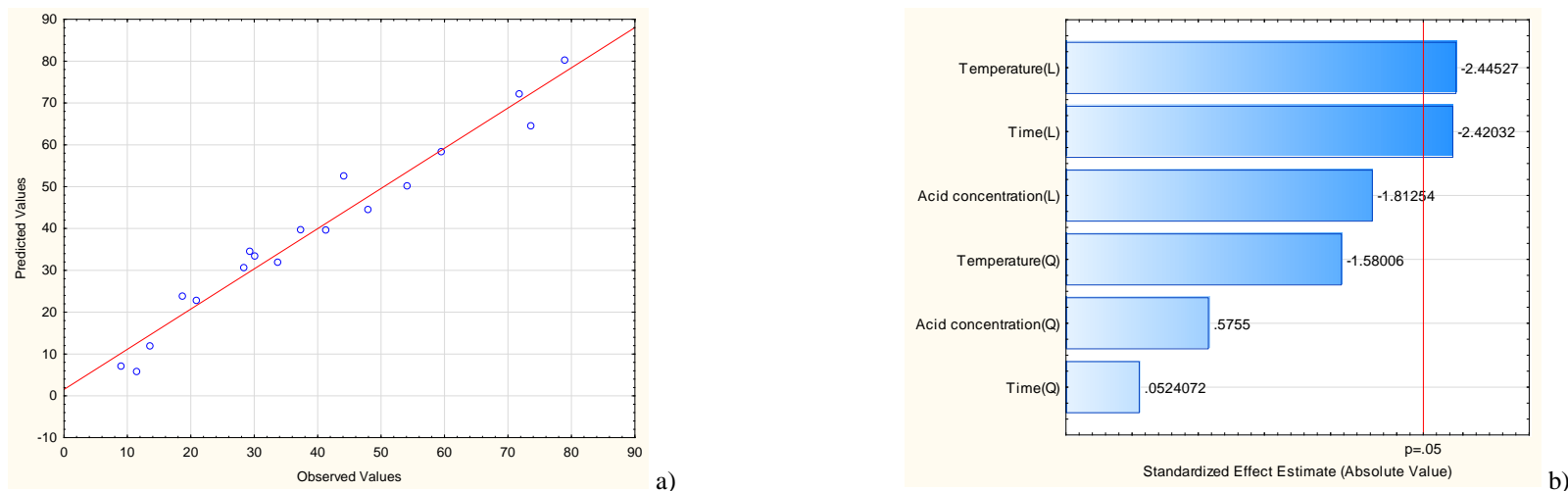


Figure 6: Observed vs predicted plot (a) and Pareto chart (b) of standardised effects of CNC yield, respectively (L values are linear values of p, and Q are quadratic values of the variables; Q values help to get the optimal values of each of the variables and the negative values are represented as positive values

Table 8
Regression analysis of a full second-order polynomial model for optimisation of CNC yield

Factor	Dependent variable = Yield; $R^2 = 0.96$; Adjusted $R^2 = 0.94$; MS Residual = 28.10					
	Regression coefficient	Standard error	T	P	-95% Confidence limit	+95% Confidence limit
Mean/intercept	44.294	9.580	4.62	0.001703	22.20	66.38
Temperature (°C)(L)	148.469	15.753	9.42	0.000013	112.14	184.79
Temperature (°C) (Q)	-207.896	25.607	-8.11	0.000039	-266.94	-148.84
Acid concentration (%) (L)	-0.258	0.494	-0.52	0.616067	-1.39	0.88
Acid concentration (%) (Q)	0.005	0.006	0.73	0.482595	-0.01	0.02
Time (min)(L)	-0.791	0.590	-1.34	0.216903	-2.15	0.57
Time (min)(Q)	0.061	0.040	1.49	0.173194	-0.03	0.15

Table 9
Effect estimates of a full second-order polynomial model for optimisation of CNC particle size

Factor	Dependent variable = Size (nm); $R^2 = 0.63$; Adjusted $R^2 = 0.43$; MS Residual = 364220.9					
	Effect	Standard error	T	p	-95% Confidence limit	+95% Confidence limit
Mean/intercept	907.35	145.08	6.25	0.00006	588.02	1226.69
Temperature ($^{\circ}$ C) (L)	-929.33	380.05	-2.44	0.03251	-1765.83722	-92.8421451
Temperature ($^{\circ}$ C) (Q)	-471.24	298.24	-1.58	0.14239	-1127.68052	185.188775
Acid concentration (%) (L)	-669.62	369.44	-1.82	0.09725	-1482.76018	143.507106
Acid concentration (%) (Q)	180.96	314.45	0.57	0.57653	-511.1375	873.072052
Time (min) (L)	-862.54	356.37	-2.42	0.03398	-1646.92445	-78.1671636
Time (min) (Q)	16.75	319.61	0.05	0.95914	-686.714742	720.214827

Table 10
ANOVA of a full second-order polynomial model for optimisation of CNC particle size

Factor	Dependent variable = Size (nm); $R^2 = 0.63$; Adjusted $R^2 = 0.43$				
	SS	Df	MS	F	p
Temperature ($^{\circ}$ C) (L)	2177803.78	1	2177803.78	5.974	0.032
Temperature ($^{\circ}$ C) (Q)	909308.48	1	909308.48	2.493	0.142
Acid concentration (%) (L)	1196576.78	1	1196576.78	3.285	0.097
Acid concentration (%) (Q)	120630.05	1	120630.05	0.331	0.576
Time (min) (L)	2133594.75	1	2133594.75	5.853	0.033
Time (min) (Q)	1000.33	1	1000.33	0.002	0.959
Temperature ($^{\circ}$ C) L+Q	3009170.62	2	1504585.31	4.130	0.045
Acid concentration (%) L+Q	1346620.71	2	673310.35	1.848	0.203
Time (min) L+Q	2166779.84	2	1083389.9	2.974	0.092
Error	4006430.13	11	364220.92		
Total SS	10877368.4	17			

Less deviation from the straight line indicates less deviation from the predicted value. It is a satisfactory correlation between the experimental data and the predicted data. For particle size of the extracted CNC checkpoint, the result was found to be within limits. This is helpful in establishing the validity of the generated equation and to describe the domain of model applicability. A linear pattern observed in this plot suggests that there was no discrepancy in the experimental data. Residuals displayed randomness in scattering and suggested that the variance of the original observation was constant.

Pareto chart (Fig. 8) results indicate that temperature is the first most influencing variable and time is the second one among the chosen parameters, as indicated by the p values. The significance of each coefficient

was determined using the Pareto chart and p value in Table 11. It was evident that the variable with the largest effect was the linear term of temperature, followed by quadratic temperature and the linear time. The factor t-test value (2.44) and p value (0.032) corresponding to linear temperature was the significant factor. According to the t and p value of temperature and time, the quadratic values of both time and temperature did not have any statistical significance. The linear effect of time was found to have a p value > 0.05, indicating the broad range effect of the variable on the CNC particle size. Square values of the variables are used to indicate their quadratic effects, so as to get the curvature in the response surface graphs and to get the optimal value for each variable.

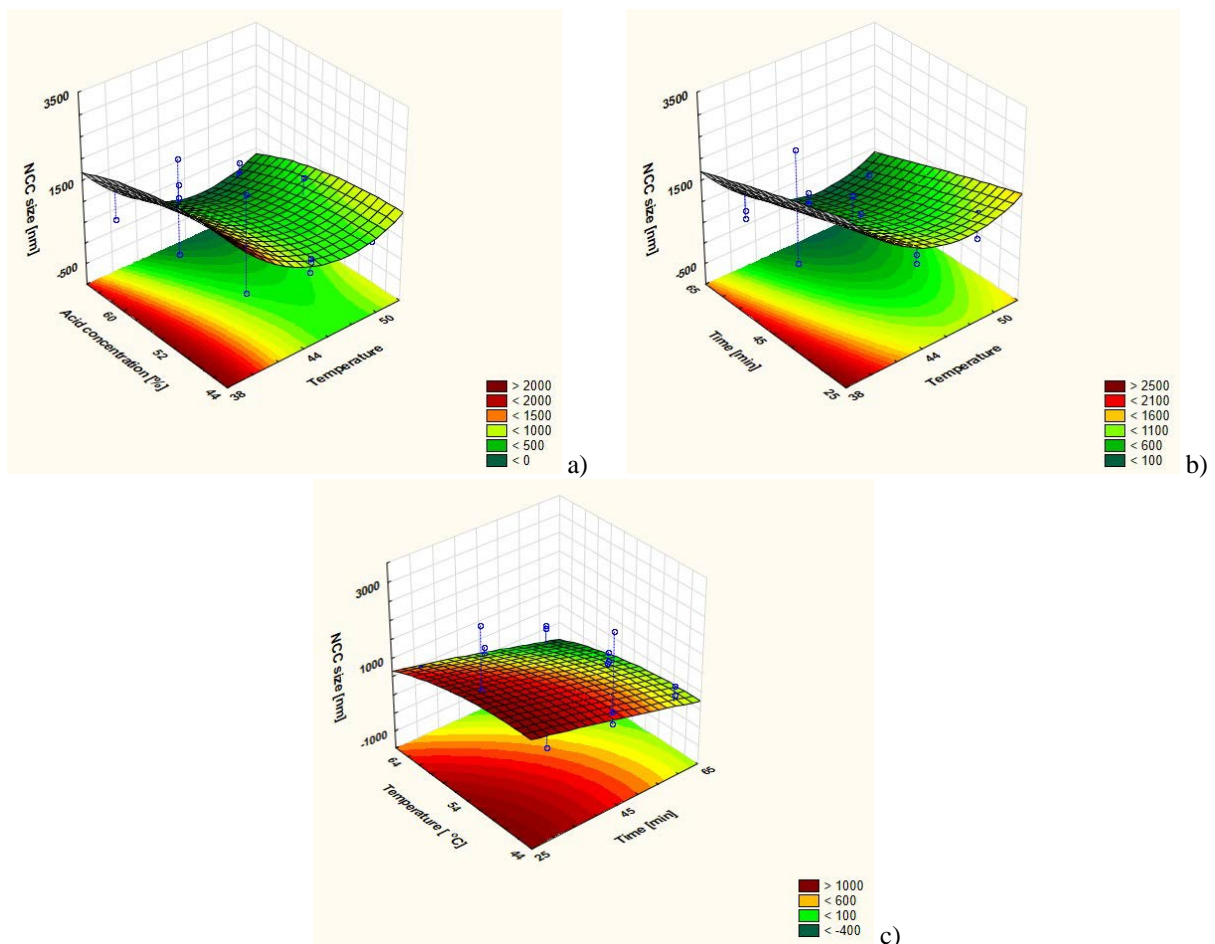


Figure 7: Response surface plot showing the effect of (a) acid concentration and temperature, (b) time and temperature and (c) acid concentration and time on CNC particle size

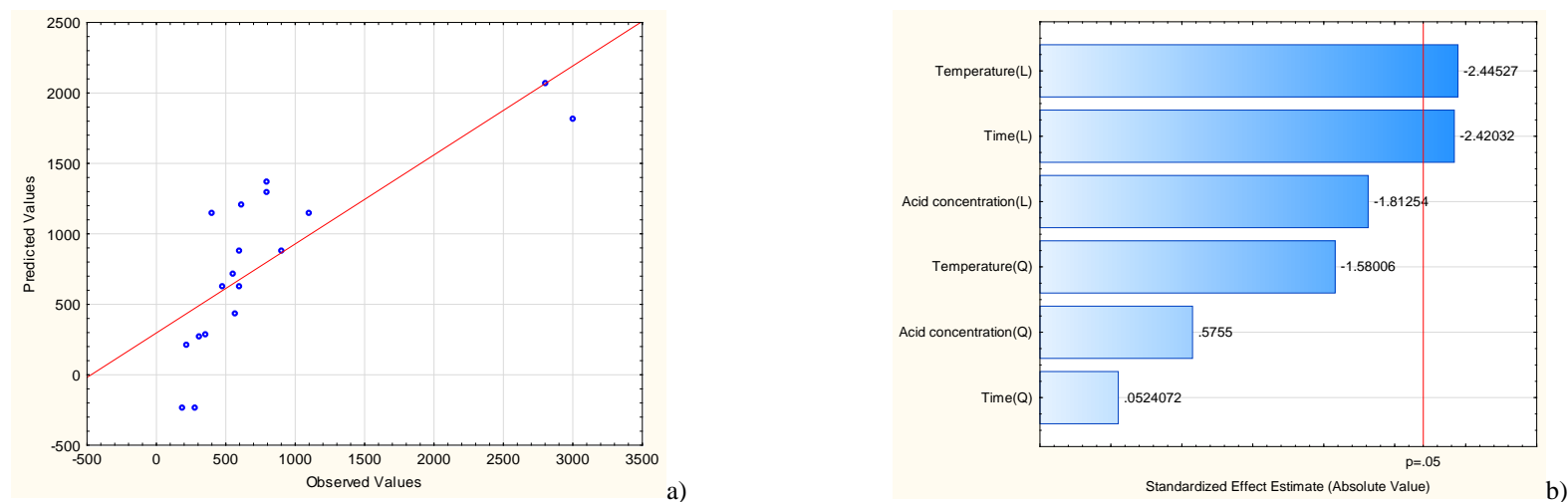


Figure 8: Observed vs predicted plot (a) and Pareto chart (b) of standardised effects, respectively

Table 11
Regression analysis of a full second-order polynomial model for optimisation CNC particle size

Factor	Dependent variable = Size (nm); $R^2 = 0.63$; Adjusted $R^2 = 0.43$					
	Regression coefficient	Standard error	t	P	-95% Confidence limit	+95% Confidence limit
Mean/intercept	40588.23	27657.47	1.46	0.17	-20285.44	101461.914
Temperature ($^{\circ}$ C) (L)	-1789.41	1075.44	-1.66	0.12	-4156.45	577.612466
Temperature ($^{\circ}$ C) (Q)	18.84	11.92	1.58	0.14	-7.40	45.1072208
Acid concentration (%) (L)	165.58	347.06	0.47	0.64	-598.29	929.457759
Acid concentration (%) (Q)	-1.80	3.14	-0.57	0.57	-8.73	5.111375
Time (min) (L)	-22.05	129.60	-0.17	0.86	-307.30	263.200062
Time (min) (Q)	-0.07	1.42	-0.05	0.95	-3.20	3.05206552

Table 12
Critical values of a full second-order polynomial model for optimisation of extracted CNC

Factor	Observed minimum	Critical values	Observed maximum
Acid concentration (%)	45	45	65
Temperature (°C)	40	45	50
Time (min)	30	60	60

Critical value of the optimisation process

The critical value of the process is calculated based on its simultaneous optimisation (the aim being to increase the yield of CNC and decrease the particle size of extracted CNC). The critical values for the optimisation of the extracted CNC, given by the software, are as follows: temperature of 45 °C; acid concentration of 45% and time of 60 min, with a percentage yield of 56.3% and particle size of the extracted CNC of 360 nm (Table 12). The influential effect of input variables on the extraction process was represented using response surface plots, as illustrated in Figures 5 and 7.

CONCLUSION

The use of ultrasonication as a pretreatment step for cellulose hydrolysis reactions was evaluated and the results obtained are quite promising. SEM and TEM images revealed changes in the cellulose morphology upon ultrasonication due to cavitation within the cellulose fibril structure. The effect of ultrasonication on the cellulose structure can be summarised as follows:

- SEM confirmed cellulose fibre disruption due to peeling of fibril layers and the formation of a fibril web. Longer pretreatment revealed the formation of CNC;
- The highest yield of CNC (79.54%) was obtained when the ultrasonication pretreatment interval time was 45 minutes;
- XRD results revealed that a slight decrease of the crystallinity index occurred with an increase in sonication time;
- TEM results showed that the CNC size was affected by the different pretreatment times, *i.e.*, long pretreatment times led to short length and higher width dimensions of the CNC fibres.

The Box Behnken design experiments showed that:

- The value of the adjusted determination coefficient was $R^2 = 0.94$, confirming that the model was highly robust;
- Time was the most significant dependent variable, followed by acid concentration;
- The critical values for optimisation of the CNC extracted process were as follows: temperature of 45 °C, acid concentration of 4% and reaction time of 60 min, resulting in CNC yield of 56.3% with a particle size of 360 nm.

Future work will entail a cost–benefit analysis on the ultrasonication pretreatment time to ascertain the optimal and feasible pretreatment time.

REFERENCES

- ¹ A. Jabbar, “Sustainable Jute-Based Composite Materials: Mechanical and Thermomechanical Behaviour”, Springer, Berlin Heidelberg, Germany, 2017, pp. 71-84.
- ² R. K. Chandler, A. Singh and K.-E. L. Eriksson, in “Biotechnology in the Pulp and Paper Industry”, edited by K.-E. L. Eriksson, Springer, Berlin Heidelberg, Germany, 1997, pp. 45-125.
- ³ Y. Nevo, N. Peer, S. Yochelis, M. Igarria, S. Meirovitch *et al.*, *RSC Adv.*, **5**, 7713 (2015).
- ⁴ A. Khan, R. A. Khan, S. Salmieri, C. Le Tien, B. Riedl *et al.*, *Carbohydr. Polym.*, **90**, 1601 (2012).
- ⁵ S. Elumalai, A. Bhumica, M. R. Troy and S. S. Rajender, *Carbohydr. Polym.*, **150**, 286 (2016).
- ⁶ X. M. Dong, J. F. Revol and D. G. Gray, *Cellulose*, **5**, 19 (1998).
- ⁷ S. C. Beck, R. Maren and D. G. Gray, *Biomacromolecules*, **6**, 1048 (2005).
- ⁸ W. Li, W. Rui and L. Shouxin, *BioResources*, **6**, 4271 (2011).
- ⁹ S. P. Mishra, A. S. Manent, B. Chabot and C. Daneault, *BioResources*, **7**, 422 (2011).
- ¹⁰ S. S. Wong, S. Kasapis and Y. M. Tan, *Carbohydr. Polym.*, **77**, 280 (2009).
- ¹¹ J. X. Sun, R. C. Sun, X. F. Sun and Y. Q. Su, *Carbohydr. Res.*, **339**, 291 (2004).

¹² R. Rohaizu and W. D. Wanrosli, *Ultrason. Sonochem.*, **34**, 631 (2017).

¹³ N. Ngadi and N. S. Lani, *J. Teknol.*, **68**, 35 (2014).

¹⁴ S. Park, J. O. Baker, M. E. Himmel, P. A. Parilla and D. K. Johnson, *Biotechnol. Biofuels.*, **3**, 10 (2010).

¹⁵ L. G. Segal, J. J. Creely, A. E. Martin and C. M. Conrad, *Text. Res. J.*, **29**, 786 (1959).

¹⁶ X. Wang, F. Guizhen, H. Chunping and D. Tianchuan, *J. Appl. Polym. Sci.*, **109**, 2762 (2008).

¹⁷ M. Ioelovich, *ISRN Chem. Eng.*, **2012**, 1 (2012).